Memory effects in a submicrometre metal-dielectric composite system

2002 J. Phys.: Condens. Matter 14 5355

(http://iopscience.iop.org/0953-8984/14/21/310)

INSTITUTE OF PHYSICS PUBLISHING JOURNAL OF PHYSICS: CONDENSED MATTER

J. Phys.: Condens. Matter **14** (2002) 5355–5366 PII: S0953-8984(02)32648-1

Memory effects in a submicrometre metal–dielectric composite system

A B Pakhomov, S K Wong, S T Hung, S G Yang and C Y Wong

Magnetics Innovation Center (MAGIC), Materials Characterization and Preparation Facility, Hong Kong University of Science and Technology, Clear Water Bay, Kowloon, Hong Kong, People's Republic of China

Received 14 January 2002
Published 16 May 2002
Online at stacks.iop.org/JPhysCM/14/5355

Abstract

Electrically driven switching of resistance states is observed in a system prepared by depositing Co and Cu layers in trenches of widths 50–500 nm in SiO_2, followed by application of a controlled high-density current. This 'forming' process leads to both an increase of resistance and a transition from metallic conduction to activated tunnelling. In the resulting system, the value of resistance can be switched reversibly by positive or negative voltage. After applying a positive bias >1.3 V the low-bias resistance decreases, while after applying a negative bias of the same value it increases. The resistance ratio between the high-resistance and low-resistance states of the system is in the range $\sim$1.5–6. A possible interpretation of the observed phenomena is discussed.

1. Introduction

Several approaches have been employed to develop new non-volatile memories controlled by voltage or current. Considerable progress has been achieved in the studies on resistance switching due to reversible phase-change transformations between crystalline (conductive) and amorphous (resistive) states in chalcogenide alloys by appropriate Joule heating and cooling [1, 2]. Current-controlled resistance change related to phase transition has been also observed in crystalline VO_2 [3]. Field-induced reversible reorientation of molecules in a polymer can lead to controllable resistance switching due to the order–disorder transition [4]. Electrical polarity-dependent switching was observed in V/a-Si/Cr structures after 'forming' by initial application of high voltage [5–7]. Diffusion processes result in a granular metal–insulator medium with hopping conduction. The inter-particle distance, and hence resistance, is controlled by the external field [5–7]. The memory effect in metal–insulator–metal structures with transition-metal-doped insulating perovskites has been discussed in [8–10]. These structures also require initial forming by relatively high voltage, which considerably reduces the resistance due to the creation of conducting filaments, before the system is able to display

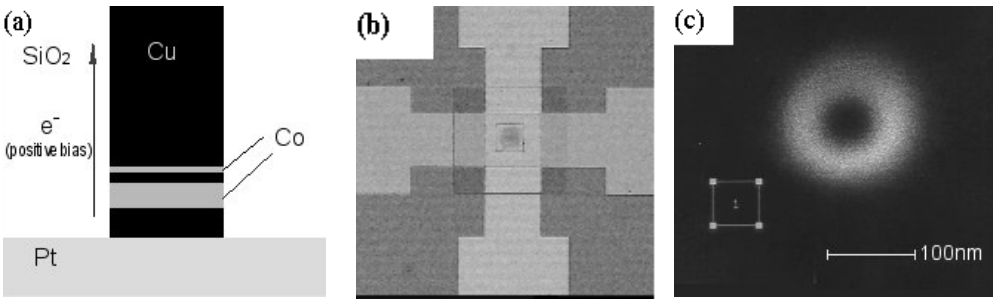

Figure 1. (a) Schematic cross section of the device prior to 'forming'; the positive current corresponds to electron flow from the bottom to the top of the pillar. (b) Crossing electrodes; the large transparent square is the SiO_2 layer. (c) The surface of silica with a trench (via).

switching and memory effects. The memory effects and switching have been explained by the storage of charges in traps (high-resistance state) and their release (low-resistance state) under the applied bias [10]. The number of electrons in the traps affects the tunnelling via a wide impurity band in the insulating gap [10, 11]. Earlier work on memory effects in insulators is reviewed in [8–10]. In several magnetic memory designs, based on either giant magnetoresistance or tunnelling magnetoresistance [12–15], the resistance state is switched due to magnetization reversal of one of the magnetic layers in the system. In certain structures this can be achieved by direct application of spin-polarized current through the sample ('spin transfer') [14, 15].

In this paper, we report on resistance switching and memory effects in a submicrometre metal–dielectric system. Co/Cu/Co layers were deposited into SiO_2 trenches (vias) between a Pt electrode on the bottom and a Cu electrode on the top. Modification of the structure, associated with an increase of the resistance, was achieved by subjecting the metal column to a controlled high-density current. After this treatment, the samples acquired new interesting properties, including the possibility of switching between different resistance states by applying positive or negative bias. The I–V (V–I) curves and the temperature dependence of the resistance in the resulting devices suggest that the conduction is dominated by thermally activated tunnelling (hopping). We discuss the switching process and the memory effect in terms of the Simmons–Verderber model [11]. Preliminary results of our work were reported in [16].

2. Sample preparation

2.1. Deposition of metal column

The nominal structure of a metal column deposited in a trench (via) in silica is shown in figure 1(a). The patterns were fabricated on an oxide layer formed upon Si substrates by thermal oxidation. First, 100 nm Ti/100 nm Pt electrodes with contact pads were prepared (the vertical electrode in figure 1(b)). Then, a 140 nm thick SiO_2 layer was deposited over the bottom electrode, which is seen as the large square in the figure. Trenches in SiO_2 of dimensions 50×50, 100×100, 250×250 and 500×500 nm^2 (figure 1(c)) were etched with focused ion beams. The etching was stopped immediately on reaching the bottom electrode. A multilayer with the nominal structure of Cu(10 nm)/Co(x, x = 10 nm or 40 nm)/Cu(5 nm)/Co(2.5 nm)/Cu(5 nm) was deposited onto the 100×100 μm^2 area (the small square in figure 1(b)), including the trench openings, by e-beam evaporation. Care was

taken to ensure that there was perpendicular deposition into the trenches. After this, the top Cu electrode was fabricated. The test Cu/Co/Cu/Co/Cu films were deposited on Si wafers simultaneously with the samples for HRTEM and EDX analyses.

2.2. Forming of the electronic memory structure

Experiments were conducted on 26 samples with lateral dimensions of 50, 100, 250 and 500 nm. Voltage as a function of current (I–V) and current as a function of voltage (V–I) were studied on an HP 4156 B semiconductor parameter analyser using the four-probe method. Current sweeps with the maximum current amplitude of 100 mA were used for structure modification. In all measurements we define the bottom (Pt) electrode as the ground, so the electrons flow from the bottom to the top at a positive bias as shown in figure 1(a).

All the samples were first tested at room temperature using current sweeps with an amplitude below 5 mA. In this current range, about 85% of the samples had nearly linear I–V characteristics with resistances distributed between 1 and 50 Ω. These values are consistent with the measured resistivity of the test films, $\rho_{film} \approx 16\ \mu\Omega$ cm, and the sample dimensions. In these samples, the differential resistance, $R = \mathrm{d}V/\mathrm{d}I$, increased slightly with increasing current. The remaining 15% of the samples exhibited non-linear behaviour, which is typical of tunnelling, with the maximum resistance of about one hundred to a few hundred ohms at zero current.

Increasing the current through a device with an initially linear I–V characteristic could break the metallic conduction and cause the I–V characteristic to become non-linear, with a simultaneous sharp increase of resistance from a few ohms to hundreds of ohms. In some samples, multiple applications of currents with the amplitude of ±100 mA (the maximum current available in our setup) were needed to achieve this transformation. An example of such a transformation is shown in figure 2. The I–V curves (figure 2(a)) and the dependences of the differential resistance, $\mathrm{d}V/\mathrm{d}I$, on the current (figure 2(b)) of the sample are plotted for several steps of the transformation denoted as 1–4, where 1 is the first measurement. After reaching the final step, 4, the structure generally stabilized, and further measurements reproduced this curve (except for the positions of the switching events, which reproduced statistically). After the breakdown, a clear hysteresis was observed in the I–V characteristics. The resistance at the small current assumes two distinctly different values. The direction of the sweep is shown by arrows. Apparently, the 'forming' process may be caused by some combination of the Joule heating, diffusion, electromigration, melting, surface tension and magnetic pressure on the metal column at high current densities.

3. Results

3.1. Memory effects and switching

Both in the initially non-linear samples and in samples transformed to the non-linear state by application of large currents, as described in the previous section, the I–V curves are hysteretic when the sweep amplitude is larger than ∼10 mA. The threshold character of the switching process becomes more apparent when measurements are made with voltage as an independent variable. Figure 3(a) shows the V–I loops measured on four samples of different diameters. The differential resistance, $\mathrm{d}V/\mathrm{d}I$, as a function of voltage is plotted in figure 3(b) for one of the samples. To avoid further modification of the structure, the sweep amplitude is chosen so that the current is smaller than 90 mA in all measurements. Qualitatively, all samples behave in a similar way, independent of sample diameter and the values of the high and low resistances,

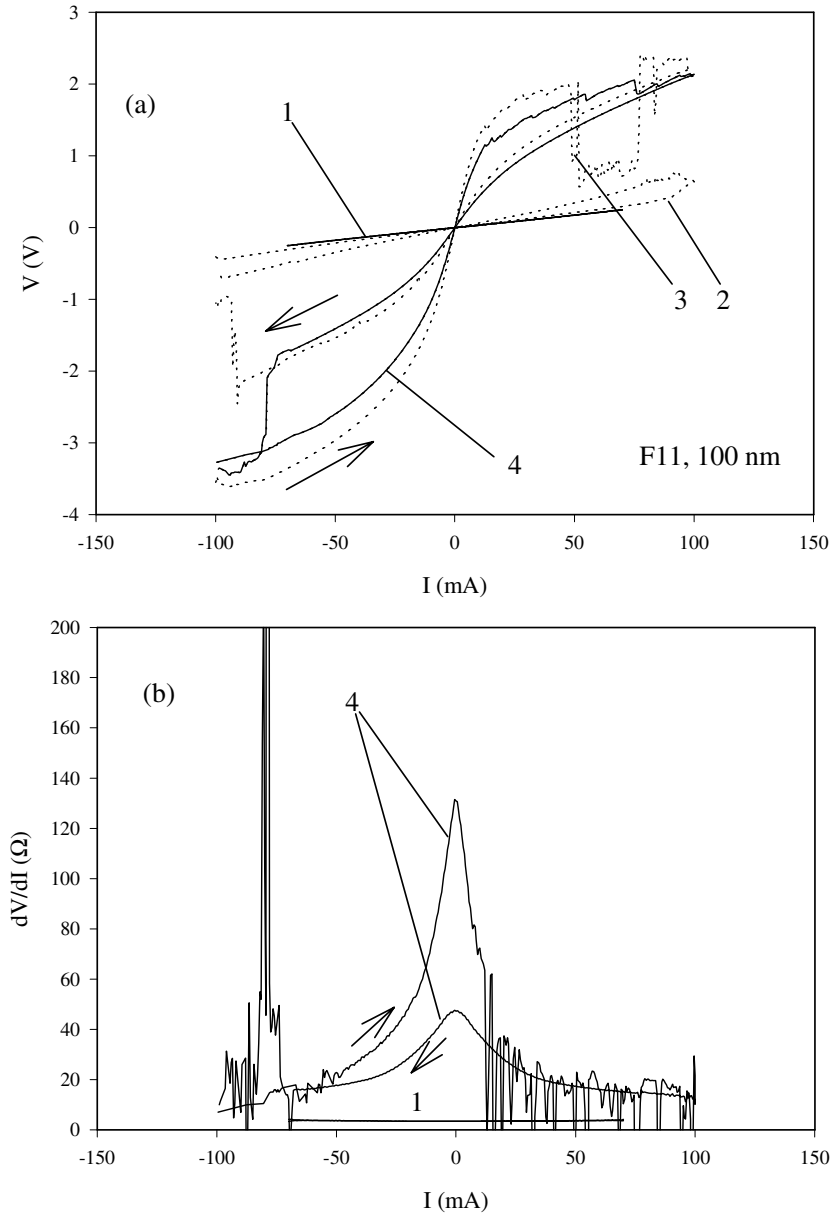

Figure 2. Interruption of the metallic conduction under the action of a sequence of current cycles: (a) voltage versus current; (b) differential resistance, $\mathrm{d}V/\mathrm{d}I$, versus current. The consecutive stages of the transformation are denoted with the numbers, where 1 is the first measurement.

R_{high} and R_{low}, at zero voltage. At negative bias larger then V_{write} the system is switched to the high-resistance mode, while at the positive bias V_{erase} the system returns to the low-resistance mode. Moreover, we notice that $V_{erase} \approx |V_{write}|$ and that this value is universal ($\sim$1.3 V) for samples of different dimensions and different zero-voltage resistances (some statistical deviations from this value are observed). We conclude that the applied voltage rather than the current is the physical parameter that controls the switching behaviour. We also observe

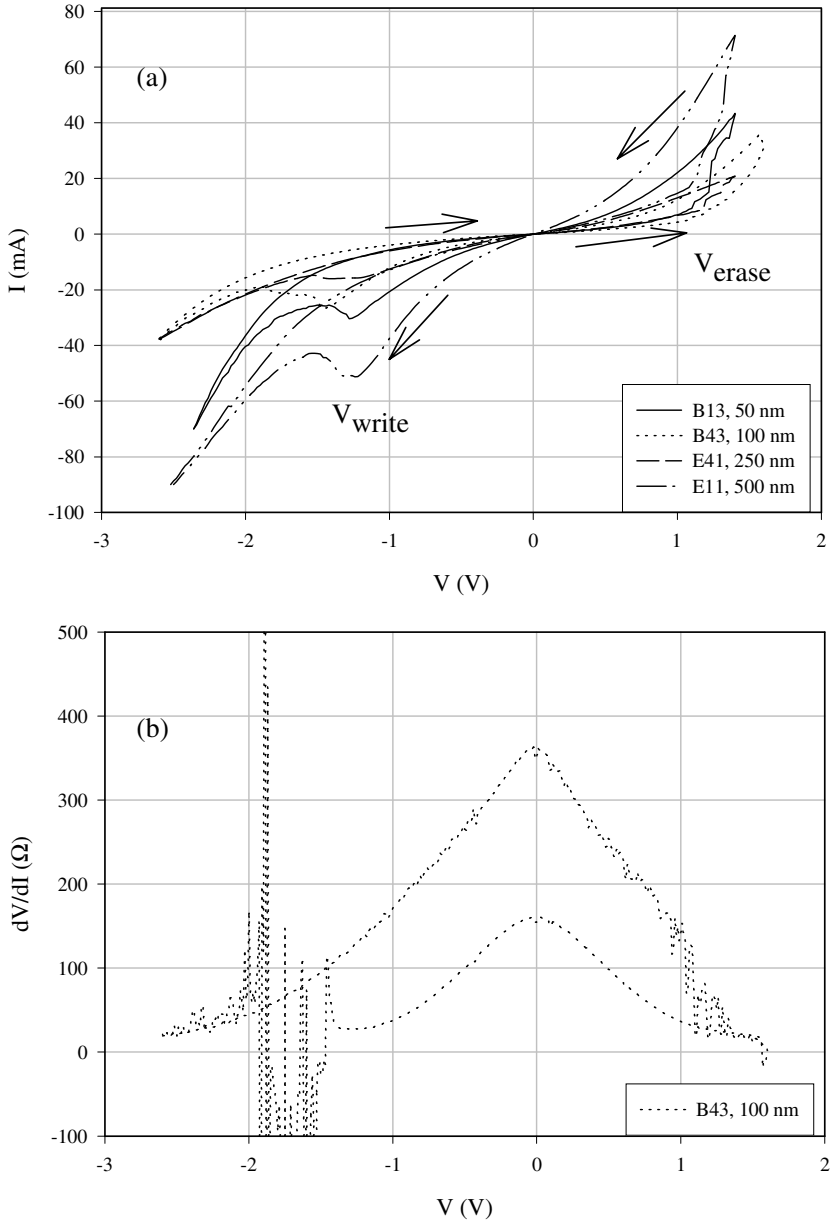

Figure 3. Memory effects and switching in four samples of different diameters: (a) current; (b) differential resistance, $\mathrm{d}V/\mathrm{d}I$, as a function of the applied bias.

staircase behaviour of the current as a function of voltage at biases greater than the threshold. The system remains in either the low-resistance state or the high-resistance state for at least several days (the timescale that we checked), without any change in resistance.

Based on the statistics collected on 26 samples of different dimensions, the values of R_{high} are widely distributed between 50 and 400 Ω and the values of R_{low} are between 20 and 150 Ω for the maximum switching voltage which would not lead to further irreversible structural

changes. The R_{high}/R_{low} ratios are in the range between 1.5 and 6 and decrease on average with increasing sample diameter. We also measured the magnetoresistance of a few samples at room temperature in an external magnetic field up to 10^4 Oe, both in the low-resistance and in the high-resistance states. The change of resistance in the magnetic field was found to be negligible compared with the difference between R_{high} and R_{low}, which allowed us to exclude magnetic memory effects.

The resistive state of the sample can be changed by application of short positive or negative electric pulses. As the duration of the pulse decreases, the voltage required to switch the device increases. The duration of the pulse becomes important in the nanosecond range. In the experiments described here, the sample was first switched to the high-resistance state by a negative DC current of −50 mA. The sample was then exposed to the action of single rectangular voltage pulses with positive or negative polarity, with durations in the range 0.1–10 ns and a fixed amplitude of 7.5 V. DC resistance was measured at a small constant current after each pulse. Similar experiments were performed after the sample had been switched to its low-resistance state by a DC current of +50 mA. Based on the static results in figure 3, one would expect that a positive pulse would decrease the resistance while a negative pulse would increase the resistance, which is indeed observed in the experiments. The results for two of a series of 12 samples tested are shown in figures 4(a) and (b). The resistance after application of a positive pulse is depicted by open symbols, while that after a negative pulse is depicted by filled symbols. Triangles and circles correspond to the switching starting from a high-resistance state and a low-resistance state, respectively. The high and low levels of resistance in the static switching experiments are shown with horizontal solid and dashed lines. The other lines are guides to the eye. Starting the experiment from R_{high}, the minimum time required for a measurable change of resistance is about 0.3 ns when $R_{high} = 204\ \Omega$ (figure 4(a)), and <0.2 ns when $R_{high} = 117\ \Omega$ (figure 4(b)). Based on the data from the 12 tested samples, with R_{high} up to 400 Ω, this correlation between the high resistance and the switching time seems to be a general tendency. Switching that starts from the low-resistance state is much slower. The minimum necessary time is ∼2 ns in figure 4(a) and ∼1 ns in figure 4(b). At $\tau = 10$ ns the switching efficiency is almost the same as that in the static regime.

3.2. Temperature dependence of resistance

Resistance was measured as a function of temperature with the temperature sweeping at a constant rate of 3 K min^{-1}, in the range 5–300 K, at a constant current. The value of the current was chosen so that the voltage across the sample did not exceed 1 mV at any temperature. Resistance was almost independent of voltage below 1 mV. The initial resistance of a sample with a linear I–V characteristic increases almost linearly with temperature at $T > 25$ K and saturates at a constant value at low temperatures, exhibiting a typical metallic behaviour. The dependences are dramatically different in non-linear samples with memory effects. Figure 5(a) shows the temperature dependence of the resistance for three typical samples, in both the high-resistance and low-resistance states. The state of the device was switched at 300 K by application of the bias $|V| > 1.3$ V of appropriate polarity. As seen in figure 5(a), the value of resistance increases rapidly with decreasing temperature (notice the logarithmic scale of the resistance). At the same time, while resistance diverges at low temperatures in the most resistive sample B13, in the sample with the smallest resistance, E43, the divergence is not apparent in the investigated temperature range ($T > 5$ K).

Non-linear V–I curves (figure 3(a)) and the large increase in resistance with decreasing temperature (figure 5(a)) suggest that thermally activated tunnelling, or hopping, in a narrow

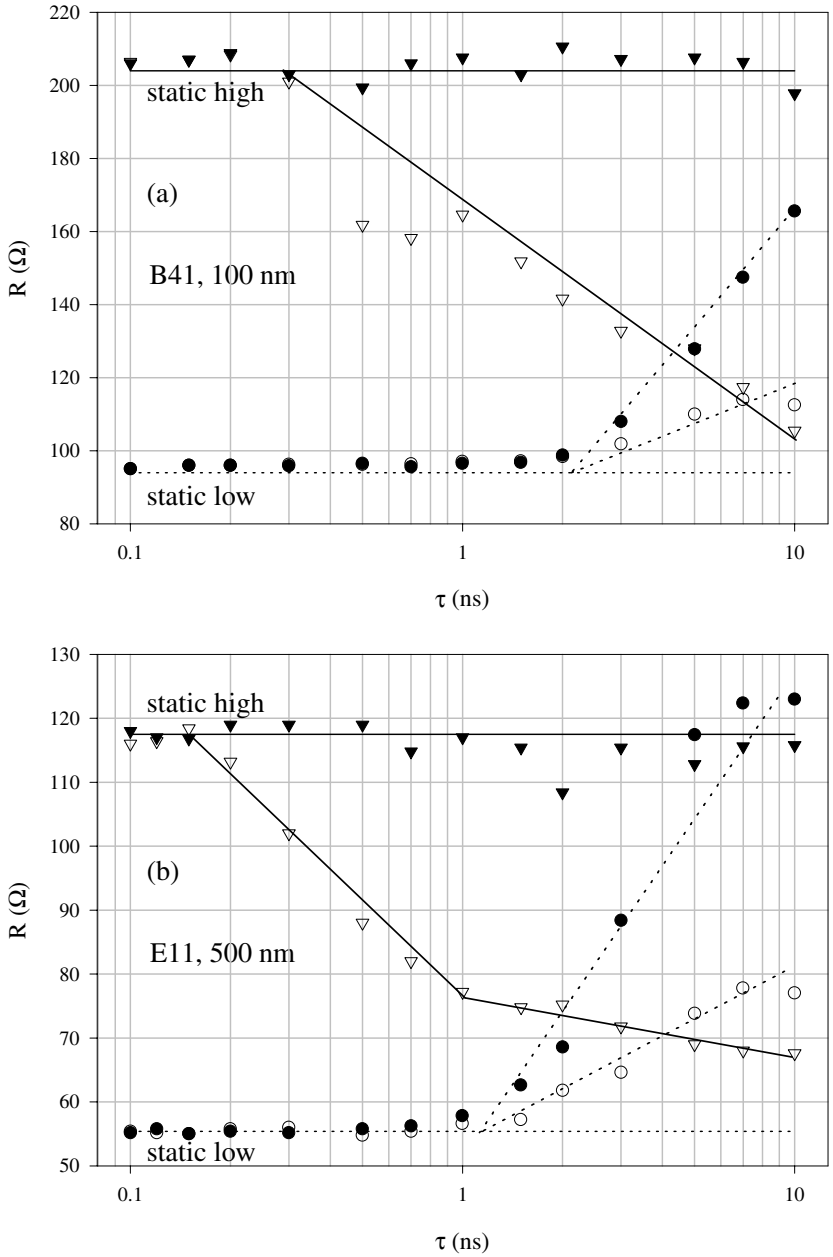

Figure 4. Dependences of resistance on the voltage pulse duration upon application of positive and negative 7.5 V pulses in two samples. Triangles: the sample is initially in the high-resistance state. Circles: the initial state is the low-resistance state (after application of DC current—50 mA). Open symbols—after positive pulse; filled symbols—after negative pulse. The horizontal lines are the levels of the DC high (solid) and low (dashed) resistance; other lines are guides to the eye.

dielectric gap is the dominating mechanism of conduction in the system. Here we rely on an analogy with the properties of granular metal–dielectric composites confined to a narrow gap between two metal electrodes, which have been studied before [7, 17, 18]. We assume that

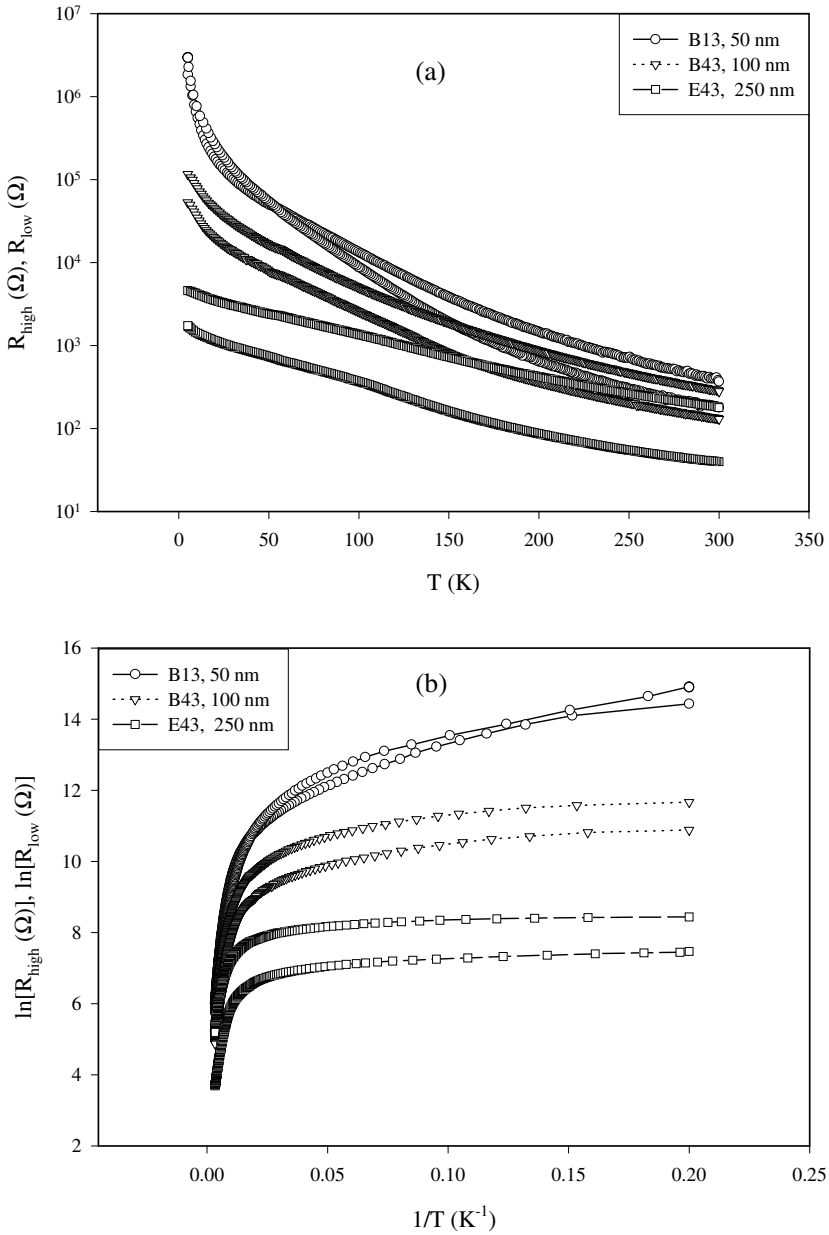

Figure 5. (a) Temperature dependence of the resistance for insulating samples measured at a low constant current, on a semi-logarithmic scale, in both the high-resistance and low-resistance states. (b), (c) Fitting plots for the hopping conduction expressions: resistance on natural logarithmic scale (b) versus inverse temperature $1/T$ (nearest-neighbour hopping model) and (c) versus $1/T^{1/4}$ (Mott's variable-range hopping in three dimensions).

hopping may occur between isolated metallic clusters, or granules, formed in the system under the action of the high-density current. Model fitting of either nearest-neighbour hopping [19], $R \sim R_0 \exp(T_0/T)$, or variable-range hopping [20], $R \sim R_0 \exp[(T_1/T)^n]$, where $n = 1/4$

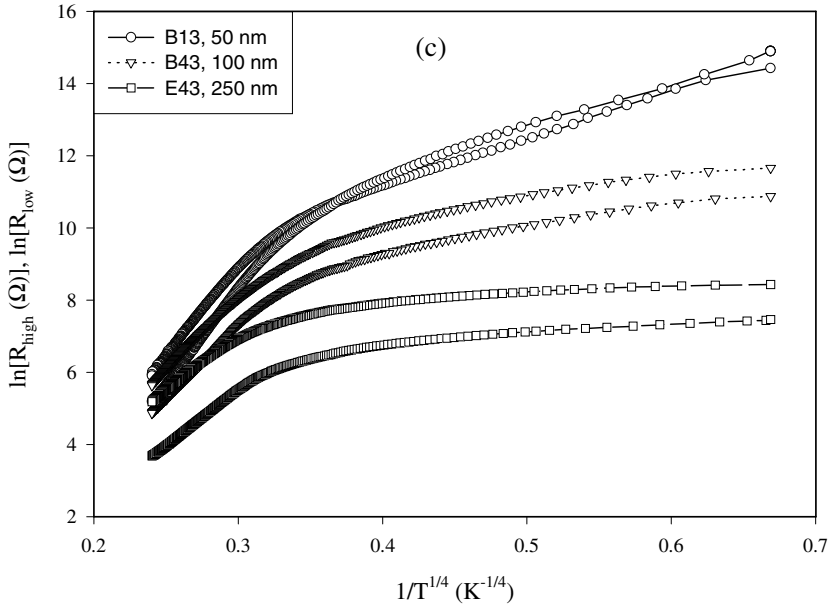

Figure 5. (Continued.)

or $1/2$, has been attempted. Figures 5(b) and (c) show the resistance on a natural logarithmic scale as a function of $1/T$ and $1/T^{1/4}$. It is seen that the experimental results do not fit with a single function in the whole temperature range 5–300 K. Assuming a simple activation at high temperatures, the constant, T_0, can be obtained from the slope of the semi-logarithmic plot of resistance as a function of inverse temperature (figure 5(b)). The resulting activation energy of the tunnelling process, kT_0, is in the range of 60–138 meV, or the constant T_0 is in the range of 430–1000 K for the different curves shown in figure 5. The activation energy, defined by this method, is always larger in the high-resistance state than the activation energy for the same sample in the low-resistance state.

4. Discussion

Except for the small fraction of devices that exhibit non-linear characteristics even at relatively low currents, it is clear that the samples initially consist of solid metal in the SiO_2 trench. However, a high-density current modifies the structure such that, in the final state, the transport is apparently by thermally activated tunnelling. At a current of 100 mA, the current density in the trench is as high as $\sim 4 \times 10^9$ A cm^{-2} for a 50 nm sample and $\sim 4 \times 10^7$ A cm^{-2} for a 500 nm sample. At this current density, a number of physical processes can combine to cause the observed transformation. Electromigration, which is expected to be greatly enhanced in this current range [21], is one of the likely mechanisms in the formation of the new structure. In the presence of non-uniformity of the conductor, electromigration can produce voids in the direction of the current, which can lead eventually to interruption of metallic conductance. Joule heating further decreases the time to failure [21]. The thermal power released in a sample with the resistance of $\sim 10\ \Omega$ at 100 mA is of the order of 0.1 W. In a submicrometre sample, this can lead to a rapid melting and fusing. This mechanism has been considered for explanation of transformation to the hopping conduction in a percolating metal–dielectric composite [22]

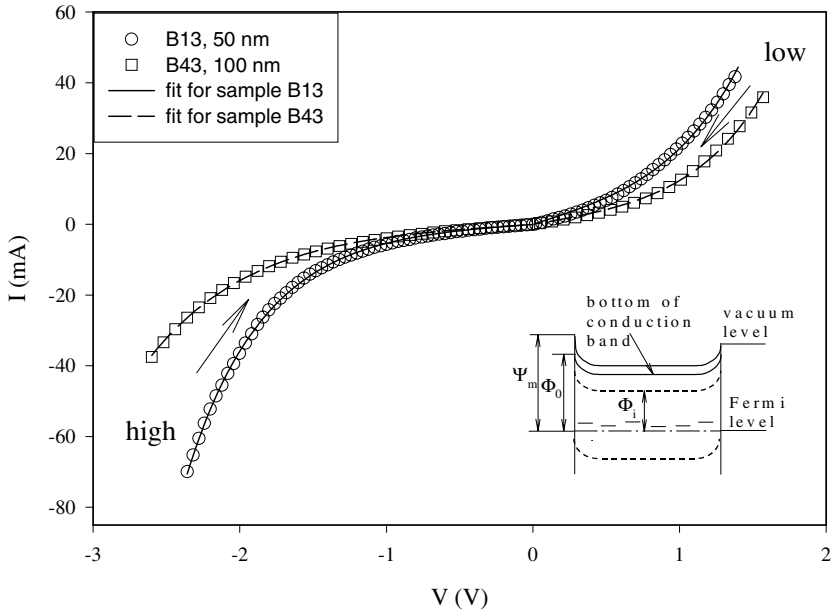

Figure 6. Fitting the typical V–I curves of the samples to the model expression $I = a^*\sinh(bV)$ [10, 11]. Symbols—experiment, curves—model. Circles—sample B13, 50 nm, squares—sample B43, 100 nm. The sweeps are from the maximum negative bias to zero (high-resistance state), and from the maximum positive bias to zero (low-resistance state), as shown with the arrows. Inset: the schematic band model of Simmons and Verderber [11].

under high-density current. The particular mechanism of the transition depends on the relative values of the increments of the instabilities caused by different factors. One can expect both considerable intermixing of metal layers and flow of amorphous SiO_2 in the conditions existing in the system during the structure formation.

We assume that, in the resulting structure, conduction is dominated by thermally activated tunnelling (hopping) between metal granules in an insulating matrix. In this case, the activation energy of conductance can be associated with the charging energy of the granule, which is $kT_0 = E_c \sim e^2/\varepsilon d$, where ε is the effective dielectric constant of the insulator ($\varepsilon \sim 4.2$ for amorphous SiO_2) and d is the metal particle diameter. In this approximation, the estimated diameters of metal clusters are in the range of approximately 2.5–6.5 nm for different samples. At low temperatures, the competition between the low charging energy and the small hopping distance leads to variable-range hopping [20]. Thus, a transition from simple activation to Mott's variable-range hopping formula, $R \sim R_0 \exp[(T_1/T)^n]$, with $n = 1/4$, can be expected, as is probably seen in figure 5(b). One should note however that the exponent $n = 1/4$ is valid only in a three-dimensional case. Because of the reduced dimensionality of the system under study, the correct exponent may be larger.

The properties of our samples, such as the hysteresis of the V–I loops and the temperature dependence of the resistance, qualitatively resemble those observed in [5–10]. The authors of [10] have considered the possibility of applying the mechanism of charge storage and release in the insulator [11] to the memory effect in $SrZrO_3$ doped with Cr. The schematic band model at zero bias [11], adapted to our case, is shown in the inset of figure 6. The dielectric with localized energy states is confined between metal electrodes with different work functions, Ψ_m. Φ_0 is the metal–insulator barrier height. A broad band of localized states in the insulator spans

between the margins, signified by the short-dashed curves, including the charging energies of granules, as signified by the long dashes. The top of the localized band is denoted as Φ_i with respect to the Fermi level. As discussed above, we assume that the circulation current in the system is mainly due to tunnelling between metal granules of the size ∼2.5–6.5 nm. The main hypothesis used to explain the memory effects in [11] is that, when sufficient voltage is applied, a negative charge can be stored in the localized levels near the top of the localized band. After removal of the bias, these charges move to the vicinity of the centre of the insulator. The barriers do not allow the charges to escape to the electrodes, while the large energy difference prevents the electrons from tunnelling to the low energy levels [11]. These stored charges reduce the field of the net positive charges in the depletion regions near the interfaces, thus decreasing the current through the interface. Storage of the charge increases the resistance, while release of the charge decreases the resistance of the system. The switching bias in this model is about the value of Φ_i, measured in electron-volts.

Neglecting the temperature effects, below the critical switching bias this model leads to a relation between current and voltage in the form $I = a^* \sinh(bV)$ [10, 11], where the constants a and b include the parameters of the interfaces. Our experimental results fit very well to the above equation. Examples of the fits are demonstrated in figure 6 for two samples: B13 (circles) and B43 (squares). The open symbols denote the experimental dependences of the current on the voltage for parts of the V–I loops without switching. The sweeps are from the maximum positive (low-resistance state) or negative (high-resistance state) voltages to zero. The solid curves indicate the fits to the Simmons–Verderber model. In a further extension of this model, the asymmetry of the switching process can be related to the asymmetry of the interface barriers between the metal electrodes and the dielectric in the gap. It is easier for the charges both to enter and to escape the top of the localized band in the insulating gap from the side of the lower barrier. In other words, the metal–dielectric tunnelling medium must be confined to a gap between two different metals with different work functions, as shown in figure 6. Simple consideration of the work functions of the metals in the system suggests that the correct result can be obtained if the lower electrode of the gap is Co and the upper electrode is Cu. We also notice different effective activation energies for conduction in different states of the same sample (figure 5), which is in line with the above description. Indeed, the activation energy can depend on the stored charge.

To conclude, we have investigated a memory system based on a metal–dielectric medium confined between metallic electrodes. The devices are made by deposition of a metal column in a SiO_2 trench and then achieving a metal–insulator transition by subjecting the column to currents of high density. Compared with the systems reported in the literature, the ‘forming’ process increases the sample resistance rather than decreases it. The observed resistance ratio between the two states of the samples could reach up to 6. The device has a nanosecond electric switching response. We suggest that conduction in this system is dominated by a mechanism similar to hopping in a granular medium and we explain qualitatively the observed switching and memory effects in terms of a charge trapping model.

Acknowledgments

We appreciate the support from the stuff at the Microelectronic Fabrication Facility (MFF), HKUST. This work was financially supported by the Hong Kong SAR Government, Innovation and Technology Commission, project AF/155/99. We would also like to thank Kevin Chen and Kwok Wai Chan, EEE Department, HKUST, for allowing us to use a microwave probe station in the pulse experiments.

References

[1] Ovshinsky S R 1968 *Phys. Rev. Lett.* **21** 1450
[2] Tyson S, Wicker G, Lowrey T, Hudgens S and Hunt K 2000 *IEEE Aerosp. Conf. Proc.* **5** 385
[3] Fisher B 1975 *J. Phys. C: Solid State Phys.* **8** 2072
[4] Gao H J, Sohlberg K, Xue Z Q, Chen H Y, Hou S M, Ma L P, Fang X W, Pang S J and Pennycook S J 2000 *Phys. Rev. Lett.* **84** 1780
[5] Hajto J, Owen A E, Gage S M, Snell A J, LeComber P G and Rose M J 1991 *Phys. Rev. Lett.* **66** 1918
Hajto J, Owen A E, Snell A J, LeComber P G and Rose M J 1991 *Phil. Mag.* B **63** 349
[6] Jafar M and Haneman D 1994 *Phys. Rev.* B **49** 13 611
[7] Hu J, Hajto J, Snell A J and Rose M J 2001 *IEICE Trans. Electron.* **84-C** 1197
[8] Beck A, Bednorz J G, Gerber Ch, Rossel C and Widmer D 2000 *Appl. Phys. Lett.* **77** 139
[9] Watanabe Y, Bednorz J G, Bietsch A, Gerber Ch, Widmer D, Beck A and Wind S J 2001 *Appl. Phys. Lett.* **78** 3738
[10] Rossel C, Meijer G I, Bremaud D and Widmer D 2001 *J. Appl. Phys.* **90** 2892
[11] Simmons J G and Verderber R R 1967 *Proc. R. Soc.* A **301** 77
[12] Parkin S S P *et al* 1999 *J. Appl. Phys.* **85** 5828
[13] Tehrani S, Chen E, Durlam M, DeHerrera M, Slaughter J M, Shi J and Kerszykovski G 1999 *J. Appl. Phys.* **85** 5822
[14] Katine J A, Albert F J, Buhrman R A, Myers E B and Ralph D C 2000 *Phys. Rev. Lett.* **84** 3149
[15] Grollier J, Cros V, Hamzic A, George J M, Jafferes H, Fert A, Faini G, Ben Yousef J and Legall H 2001 *Appl. Phys. Lett.* **78** 3663
[16] Wong S K, Pakhomov A B, Hung S T, Yang S G and Wong C Y 2001 *Symp. E: Advanced Data Storage Materials, ICMAT-2001* (Singapore)
[17] Schelp L F, Fert A, Fettar F, Holody P, Lee S F, Maurice J L, Petroff F and Vaures A 1997 *Phys. Rev.* B **56** R5747
[18] Black C T, Murray C B, Sandstrom R L and Sun S 2000 *Science* **290** 1131
[19] Nougebauer C A, Webb M B 1962 *J. Appl. Phys.* **33** 74
[20] Sheng P 1992 *Phil. Mag.* B **65** 357
[21] A Christou (ed) 1994 *Electromigration and Electronic Device Degradation* (New York: Wiley)
[22] Pakhomov A B, McLachlan D S, Oblakova I I and Virnik A M 1993 *J. Phys.: Condens. Matter* **5** 5313
Garanov V A *et al* 1991 *J. Phys.: Condens. Matter* **3** 3367